AD-A121 768 MATH MODEL FOR PREDICTION OF INFRARED SIGNATURES(U) AIR FORCE WRIGHT AERONAUTICAL LABS WRIGHT-PATTERSON AFB OH W L FOLEY AUG 82 AFWAL-TR-81-1194 1/1

UNCLASSIFIED F/G 17/5 NL

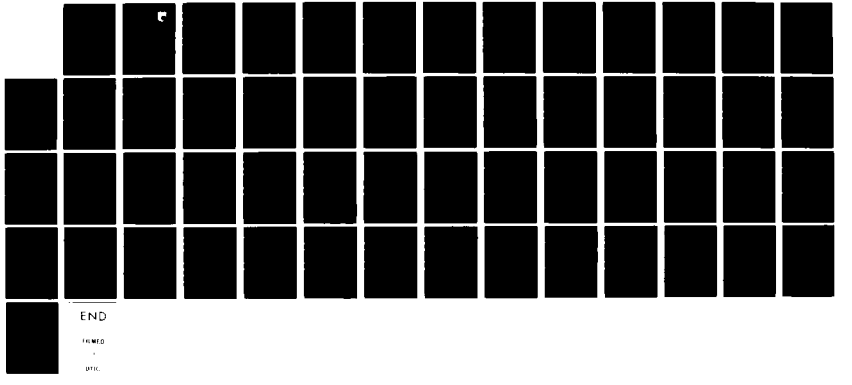

END

FILMED

DTIC

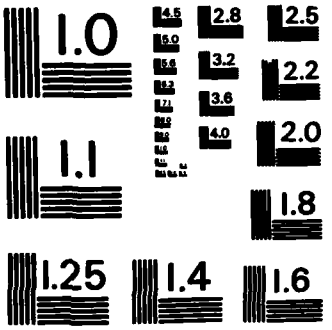

MICROCOPY RESOLUTION TEST CHART
NATIONAL BUREAU OF STANDARDS-1963-A

AFWAL-TR-81-1194

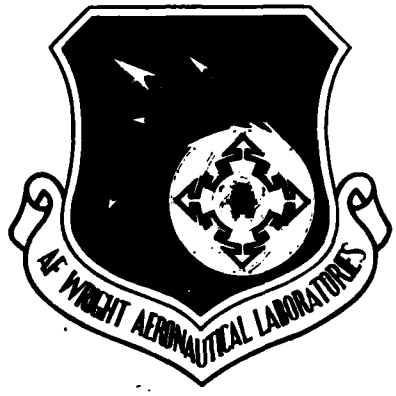

MATH MODEL FOR PREDICTION OF INFRARED SIGNATURES

William L. Foley
Sensor Evaluation Branch
Mission Avionics Division

August 1982

Final Report for Period 1 December 1980 to 30 June 1981

AIR FORCE AVIONICS LABORATORY
AIR FORCE WRIGHT AERONAUTICAL LABORATORIES
AIR FORCE SYSTEMS COMMAND
WRIGHT-PATTERSON AIR FORCE BASE, OHIO 45433

NOTICE

When Government drawings, specifications, or other data are used for any purpose other than in connection with a definitely related Government procurement operation, the United States Government thereby incurs no responsibility nor any obligation whatsoever; and the fact that the government may have formulated, furnished, or in any way supplied the said drawings, specifications, or other data, is not to be regarded by implication or otherwise as in any manner licensing the holder or any other person or corporation, or conveying any rights or permission to manufacture use, or sell any patented invention that may in any way be related thereto.

This report has been reviewed by the Office of Public Affairs (ASD/PA) and is releasable to the National Technical Information Service (NTIS). At NTIS, it will be available to the general public, including foreign nations.

This technical report has been reviewed and is approved for publication.

William L. Foley

WILLIAM L. FOLEY
Project Engineer

Edward L. Gliatti

EDWARD L. GLIATTI
Chief, System Engineering Group
Sensor Evaluation Branch

FOR THE COMMANDER

James C. Haley

JAMES C. HALEY
Chief, Sensor Evaluation Branch
Mission Avionics Division

"If your address has changed, if you wish to be removed from our mailing list, or if the addressee is no longer employed by your organization please notify AFWAL/AARE, W-PAFB, OH 45433 to help us maintain a current mailing list".

Copies of this report should not be returned unless return is required by security considerations, contractual obligations, or notice on a specific document.

Unclassified

SECURITY CLASSIFICATION OF THIS PAGE (When Data Entered)

REPORT DOCUMENTATION PAGE	READ INSTRUCTIONS BEFORE COMPLETING FORM
1. REPORT NUMBER: AFWAL-TR-81-1194	2. GOVT ACCESSION NO.: AD-A121 768
	3. RECIPIENT'S CATALOG NUMBER:
4. TITLE (and Subtitle): MATH MODEL FOR PREDICTION OF INFRARED SIGNATURES	5. TYPE OF REPORT & PERIOD COVERED: Final Report 1 Dec 80 - 30 Jun 81
	6. PERFORMING ORG. REPORT NUMBER:
7. AUTHOR(s): William L. Foley	8. CONTRACT OR GRANT NUMBER(s):
9. PERFORMING ORGANIZATION NAME AND ADDRESS: Avionics Laboratory (AFWAL/AARF) AF Wright Aeronautical Lab. AFSC Wright-Patterson Air Force Base Ohio 45433	10. PROGRAM ELEMENT, PROJECT, TASK AREA & WORK UNIT NUMBERS: P.E. 62204F 20041002
11. CONTROLLING OFFICE NAME AND ADDRESS: Avionics Laboratory (AFWAL/AARF) AF Wright Aeronautical Lab. AFSC Wright-Patterson Air Force Base Ohio 45433	12. REPORT DATE: August 1982
	13. NUMBER OF PAGES: 55
14. MONITORING AGENCY NAME & ADDRESS(if different from Controlling Office):	15. SECURITY CLASS. (of this report): Unclassified
	15a. DECLASSIFICATION/DOWNGRADING SCHEDULE:

16. DISTRIBUTION STATEMENT (of this Report)

Approved for public release; distribution unlimited.

17. DISTRIBUTION STATEMENT (of the abstract entered in Block 20, if different from Report)

18. SUPPLEMENTARY NOTES

19. KEY WORDS (Continue on reverse side if necessary and identify by block number)

Infrared
Thermal Signatures
Math Model

20. ABSTRACT (Continue on reverse side if necessary and identify by block number)

This report covers the development and implementation of math model for use in predicting surface temperature of natural and man-made features. The model utilizes time-varying environmental inputs as well as constant thermal parameters to calculate time-varying surface temperature profiles. Formulations describe solar, conductive, radiative, convective, rain and evaporative effects on air/surface boundary. Finite difference methods are used to calculate time-varying temperature of feature surfaces. Features may be elevated or coincident with

DD FORM 1 JAN 73 1473 EDITION OF 1 NOV 65 IS OBSOLETE

Unclassified

SECURITY CLASSIFICATION OF THIS PAGE (When Data Entered)

20. Abstract (Continued)

Earth's surface. Temperature or radiance from vegetative growth may also be predicted.

Model has been programmed and is operational in laboratory. Model will be incorporated into an overall laboratory program for test and validation which will commence September 1981 and, as currently scheduled, continue over a 3-year period.

Preliminary validation has been obtained using available sample data inputs. Validation at present is limited, based on data availability, to dry season only.

FOREWORD

This document was prepared by the Sensor Evaluation Branch, Systems Avionics Division, Avionics Laboratory, of the AF Wright Aeronautical Laboratories. This report describes an effort for development of a math model to predict thermal infrared signatures. The effort was performed *in support of Project 20041002 and other Avionics Laboratory programs* for prediction of the performance of E/O systems.

The principal personnel assigned to this effort were:

L. W. Crouch	AFWAL/AARF
W. L. Foley	AFWAL/AARF
A. J. Bowling	AFWAL/AARF

Mr. Leo Vroombout of the Avionics Laboratory Electro-Optical Branch was instrumental in substantiating the need for this program. Through his impetus the effort was initiated and completed.

Acknowledged is assistance in the form of consultation and support given by Dr. Jerome Clemens, Department of Geography, Wright State University; Dr. Hitchcock, Department of Mechanical Engineering, Air Force Institute of Technology; and Dr. Jim Lange, Department of Physics, Air Force Institute of Technology.

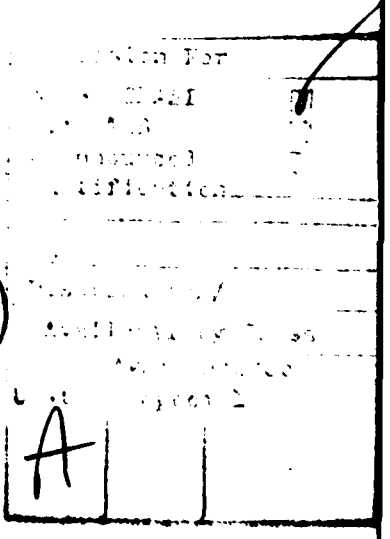

TABLE OF CONTENTS

LIST OF ILLUSTRATIONS

LIST OF TABLES

LIST OF MODEL PARAMETERS

The following list of parameters were used in the program. All energy flux is expressed in $\frac{Cal}{CM^2\text{-}MIN}$ so that the units for parameters are consistent with units for energy flux. The program expresses surface temperature in degrees Fahrenheit.

A. Special Material Parameters

Layer (K) - Number of intervals in each layer

AK(K) - Conductivity of each layer $\frac{Cal}{CM\text{-}MIN}$

D(K) - Diffusivity of each layer - $\frac{CM^2}{MIN}$

*P(K) - Density of each layer - $\frac{GM}{CM^3}$

*CM(K) - Specific heat of material - $\frac{Cal}{GM}$

ATH(K) - Thickness of interval in layer - CM

B. Constant Parameters - Non-Vegetative Features

Zo - *Surface roughness* - CM

A_s - Solar absorption - $0 \leq A_s \leq 1$

OB - Ground vegetation obscuration factor $0 \leq OB \leq 1$

C - Canopy characteristic factor

ε_o - Surface Emissivity $0 \leq \varepsilon_o \leq 1$

U - Cloud-type coefficient $.2 \leq U \leq .9$

Po - Probability of clear line of sight at Zenith (Overhead vegetation obscuration).

RI - Rainfall rate - CM/MIN

PW - Density of water - CM/CM^3

CW - Specific heat of water - CAL/GM

NLAY - Number of layers

DAY - Day of year at start of run

* Need not be specified if D(K) is input parameter since: $P(K)*CM(K) = \frac{AK(K)}{D(K)}$

ALAT - Latitude of target in degrees

T_R - Rain Temperature

DELT - Time interval between temperature update - MIN

C. Constant Parameters - Vegetation

α_{SL} - Short wavelength absorption of leaf $0 \leq \alpha_{SL} \leq 1$

α_L - Long wavelength absorption of leaf $0 \leq \alpha_L \leq 1$

ϵ_L - Emissivity of leaf

XPR - Leaf width - CM

RG - Internal diffusion resistance of leaf

D. Parameters - Active Targets

LHO - Length of surface

AL_S - Solar absorption $0 \leq AL_S \leq 1$

**Q_T - Energy input - non-solar - $\frac{CAL}{CM^2 \times MIN}$

E. The following time vary parameters must be provided at discrete time intervals.

S(t) - Total solar direct and diffuse energy - $\frac{CAL}{CM^2 MIN}$

RH(T) - Relative humidity - $0 \leq RH(t) \leq 1$

$V_M(t)$ - Wind velocity - MPH

CC(t) - Fractional cloud clover - $0 \leq CC(t) \leq 1$

$T_A(t)$ - Air temperature - °F

F. Also initial temperature values for each interval in each layer must be specified.

** Could be time varying

SECTION I

INTRODUCTION

The development of Infrared imaging systems has progressed to the degree that such systems are finding widespread application in both the air-to-air and air-to-ground combat scenarios. The typical image is a composite of signature patterns which depend upon types of features being interrogated, their physical structure, local weather conditions, atmospheric transmission and sensor system characteristics. The relative difference in signature strength which, in turn, enables the discernment of feature outlines, relates directly to differences in absolute temperatures of radiating surface. This, in turn, is influenced by the total energy exchange between radiating volume and its external environment. Signature strengths change continually in relation to each other since environmental history and energy fluxes can produce considerably differing temperature changes between radiating elements.

It follows from the above then that thermal signatures of given features can be either stronger or weaker than adjacent or nearby features, depending on time of day, season of year, etc. Key to this issue is the contrast ratio of flux intensities between some features of interest and surrounding region which is considered the background. The integration of environmental history, physical nature of target, atmospheric effects and sensor system characteristics then produces final signature patterns. This integration, in turn, adds considerable complexity to the problem of performance analysis/prediction.

The ability to perform analysis of prediction/performance of sensor system interaction with thermal environment requires some in-depth understanding of physical phenomena associated with formation of thermal patterns, transmission of signature data thru atmosphere, and sensor characteristics which produce the final image. Without the aid of sophisticated predictive technique, system performance can at best be only grossly estimated and the prediction would be largely qualitative in nature.

The goal of performance/prediction is development of methods to quantify the performance in terms of the probability of detecting, recognizing and identifying key features portrayed in the image presentation. This requires the ability to detect or recognize, bridge, wood, truck, etc. against a background of natural terrain and man-made features. The logical approach to analysis is thru a partitioning of the problem with four modules. The flow is shown in Figure 1:

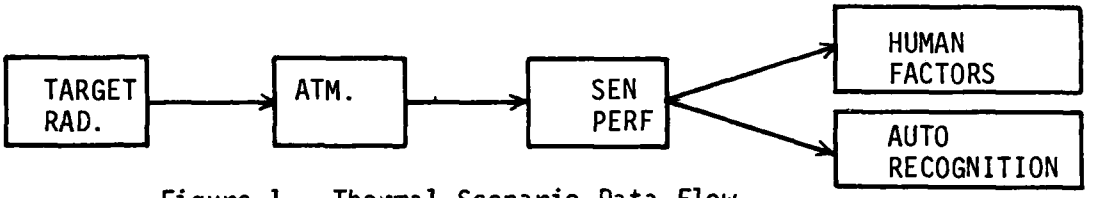

Figure 1. Thermal Scenario Data Flow

Among the four factors the most easily quantifiable is the sensor characteristic. This is reasonable since this is man-made and highly controllable, and there is extensive data available thru laboratory and field use.

The atmospheric transmission prediction is being addressed under the "Lowtran" program which, thru an extensive development history, is emerging as a reliable quantitative tool for dealing with the complex nature of this problem.

This report describes the development of a mathematical tool to predict radiance from surface features. Work conducted at Environmental Research Institute of Michigan (ERIM) (Reference 1) formed the basis for the development described herein. The math model development is complete and a FORTRAN program has been written and implemented to perform required calculations. Model utilization in a long-range program of test and investigation is anticipated.

Section II of this report discusses model capability and Section III details model development. Sections IV and V cover model implementation and analyze preliminary results.

SECTION II

MODEL CAPABILITY

The prediction of temperature/radiance of real-world features is accomplished using a mathematical model which calculates surface temperatures and/or radiance scenario features. The features are those that can easily be represented by two-dimensional or planar surfaces. However, three-dimensional features may also be modeled as a combination of planar surfaces, subject to the constraint that heat flow is one-dimensional. The one-dimensional heat flow was assumed since this type of heat flow is consistent with movement of energy flux thru features where horizontal dimensions are large in relation to thermal depth (roads, bridges, walls and roofs of buildings) and is quite reasonably traceable mathematically. Expansion of this model to allow for a three-dimensional type of heat flow can be accomplished as necessary for specialized physical configurations.

The model can predict time-dependent surface temperature for a wide variety of features with-or-without direct vegetation overlay (grass) and can account for obscuration from overhead vegetation canopy.

The types of features that can be modeled for surface temperature prediction may be divided into three categories:

1) Large massive features of indefinite extent, e.g., roads, general soil area, concrete runways, etc.
2) Small man-made targets (trucks, jeeps, etc.)
3) Vegetation

The approach to modeling those features under categories 1 and 2 requires a second-order linear partial differential equation to describe the heat diffusion process thru material constituents. An independent heat source of man-made origin may be included as part of the heat balance equation. Examples of this could include heat from a vehicle engine or from a large steampipe below the Earth's surface. The vegetation modeling uses a strictly algebraic heat balance equation.

The foregoing general categories may be subdivided or expanded as follows:

A. Large Massive Features

1) Feature elevated above Earth's surface (bridge)
2) Feature with active non-solar heat source as input
3) Non-elevated (rocks, soil, etc)

B. Small Man-Made Targets

1) Internal heat source (engine running)
2) Radiation from select portions of feature (hood, canvas back, cab)

C. Vegetation

1) Leaf temperatures of tree tops
2) Near ground vegetation (large leaves near surface or grass)
3) Underside of trees

Figures 2 and 3 illustrate typical scenarios involving both large and small vegetation and a small vehicle whose engine serves as an independent heat source. Note the partitioning of surface below the vehicle into layers based upon material composition below surface. These boundaries form volumes thru which heat exchanges are continually occurring. The heat exchange in each material volume produces the temperature profile below and at the Earth's surface during a given time interval.

Shadow effects include prediction of time-dependent differences between that portion of a surface that is currently being or had been obscured by a target vehicle and that which has been under full illumination.

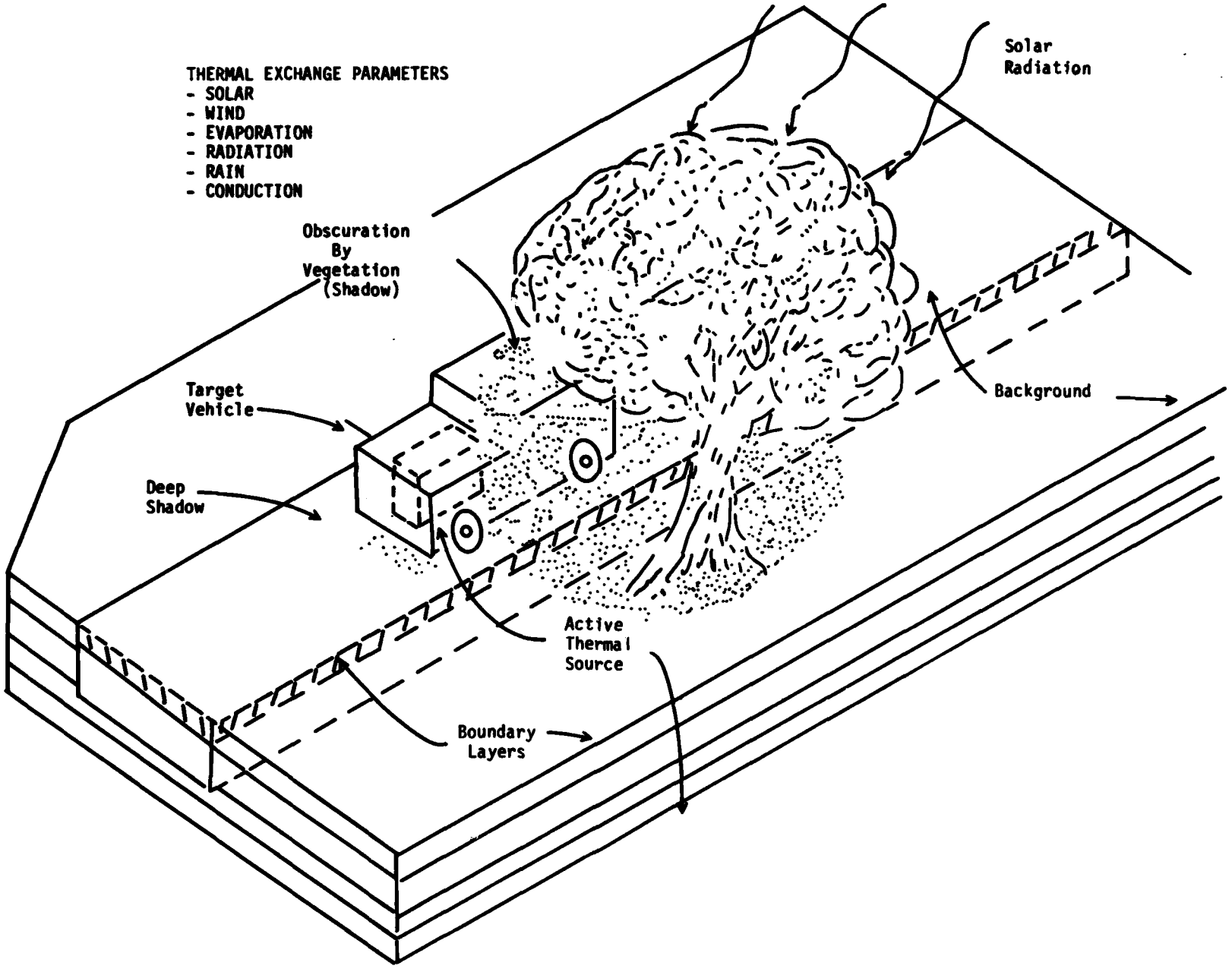

Figure 2. Target/Background Scenario

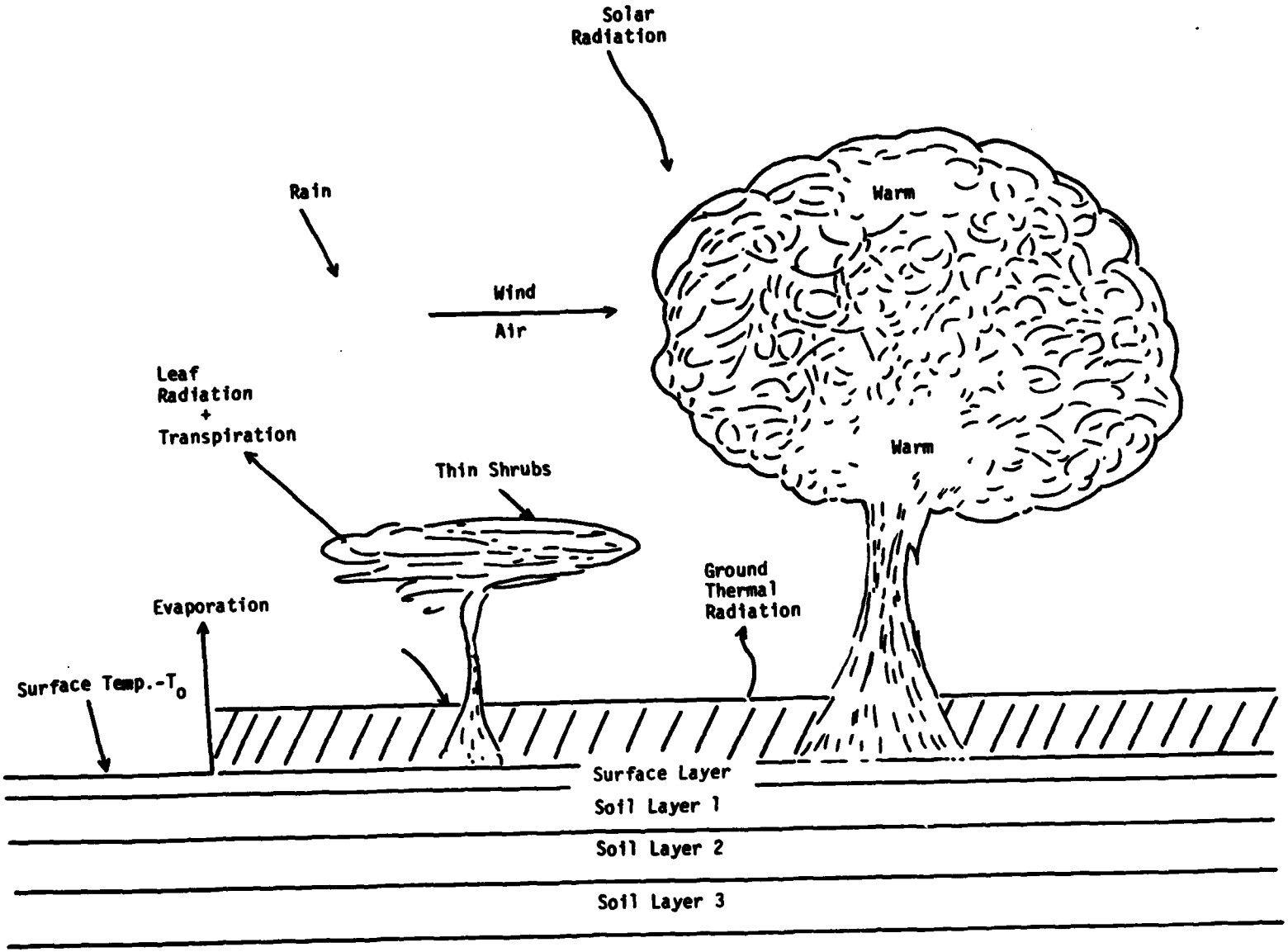

Figure 3. Thermal Exchange Mechanisms

SECTION III

DETAILED MODEL FORMULATION

1. DERIVATION - GENERAL HEAT TRANSFER EQUATIONS

As stated earlier it is assumed that the surfaces are planar and heat flux is strictly transverse to the plane of the surface. This assumption is reasonable where planar surfaces are uniformly irradiated and where surface dimensions are large in relation to thermal depth. This is consistent with roads, soil area, leaves or trees, etc.

The total environment in the heat exchange process includes the atmosphere, air/surface boundary, and the region internal to the feature itself. The air/surface boundary is the region where multiple heat exchanges acting simultaneously produce the surface temperature. The heat exchange mechanisms operating at this boundary are: (1) solar irradiation, (2) conduction to or away from surface (3) radiation transfer between the surface and atmosphere (4) convection exchange (5) rain heating or cooling, and (6) evaporation losses. Figure 4 illustrates the heat exchange process.

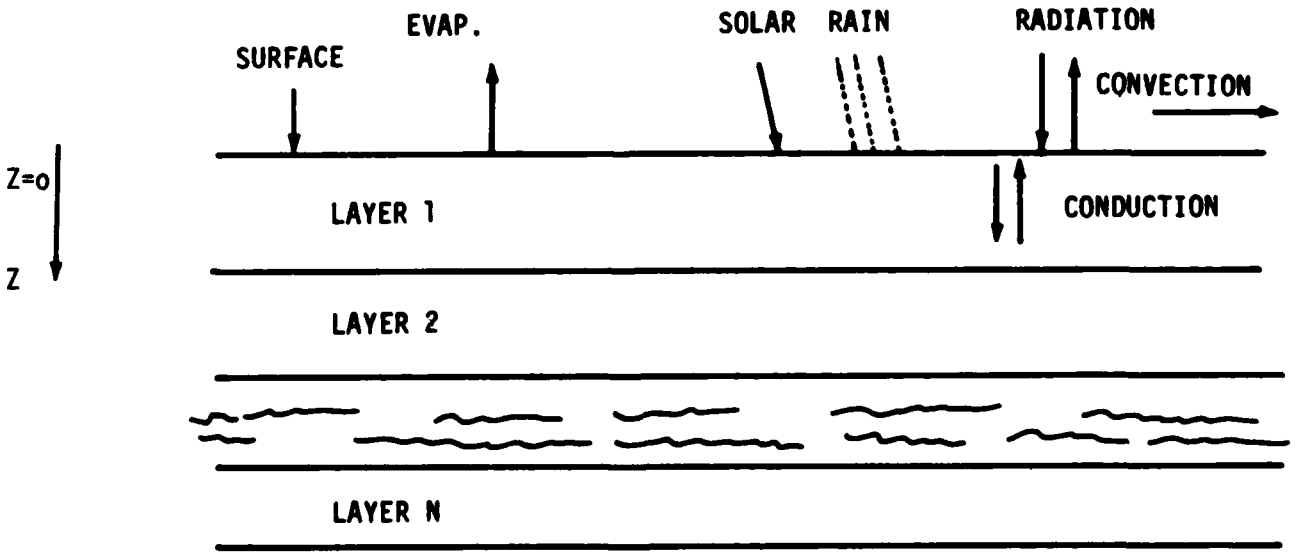

Figure 4. Terrain Cross Section - Heat Exchange

In Figure 4, the region below the surface is subdivided into layers numbered consecutively from 1 to N, starting at the air/surface boundary. The layers are assumed to be of indefinite extent horizontally. Within the volume of each layer basic thermal properties such as conductivity, diffusivity, density, etc. are considered invariant.

Considering a single layer for the moment (refer to Figure 4) the heat flow may be expressed as

$$\frac{d^2T}{dZ^2} = \frac{(P)(c)}{k} \frac{dT}{dt} \tag{1}$$

where:

P = Material density in layer
c = Heat capacity of layer
k = Conductivity of layer
T = Temperature of some point Z in layer

This equation is recognized as the classical form of heat diffusion equation for one-dimensional flow.

The equation may be solved analytically depending on temperature conditions at the upper and lower boundaries of a material substrate. The heat flow is in general dynamic i.e., continuously changing; and, in the case of the top layer, simultaneous activity involving the different heat exchange mechanisms results in complex boundary conditions. Consequently, a method known as "Finite difference" is employed which enable solution of the problem thru computer methods. The implementation of this method is based upon the subdivision of vertical heat flow path into discrete intervals and computing and updating temperature changes in these intervals during discrete time increments. Figure 5 illustrates the methodology.

The heat exchanges, operating at the surface are assumed to be interacting within a surface volume formed by a surface layer of finite depth and indefinite extent (see Figure 5). The surface layer is seen as that portion of layer 1 which is situated at the air/ground boundary. The surface layer has the same thermal properties of layer 1 but its thickness

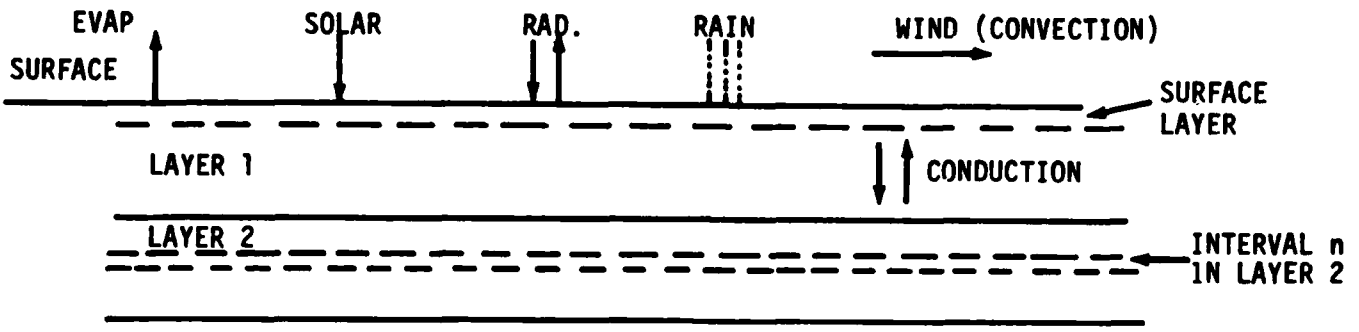

Figure 5. Terrain Cross Section - Subdivision of Layers

is generally much less than that of layer 1. Each layer, then, is subdivided into discrete intervals, each of which forms a material volume thru which heat exchanges occur. The total process is assumed to be dynamic; and where thermal inertias are large, such as the case for roads, etc., equilibrium conditions do not generally exist. Thus the net heat flow into or out of a given interval is assumed to be non-zero at all times. This, in turn, means that the temperature of each volume interval is altered, depending on whether a net quantity of heat is being added or removed from a linear volume of material at a given time.

The thickness of each interval may be chosen somewhat arbitrarily; however, there are two primary constraints which must be considered in selecting the actual values:

1) Near the boundaries, particularly the air/surface boundary, the thermal gradients tend to be relatively large in comparison with locations further removed from such boundaries. Therefore, smaller interval thicknesses are usually required in the top layer than in subsequent layers to insure that the accuracy of the final result is not compromised. Interval thickness may be considered constant in a given layer.

2) The time increment dt or Δt must also be selected with care so that, together with the number of intervals chosen, a convergence of the mathematical solution is assured.

From the foregoing discussion and Figure 5, the heat balance equation can be introduced as:

$$Q_T + \sum_{i=1}^{N} Q_i(t) = [P(K)][CM(K)]\left[\frac{\Delta T(n,K)}{\Delta t}\right][\Delta Z(K)] \qquad (2)$$

where:

$Q_i(t)$ = Value of the i^{th} heat flux component (convection, radiation, etc) into or our of interval n in layer K

$\Delta Z(K)$ = Thickness of interval in layer K

$P(K)$ = Density of material in layer K

$CM(K)$ = Specific heat of material in layer K

$\Delta T(n,K)$ = Temperature change in interval n of layer K during time interval Δt

Q_T = Independent non-solar heat source if it exists either internal or external to feature (e.g., a steampipe item below the the surface or a vehicle engine exchanging energy with the surface of the road, etc.)

Using Equation 2, the value of heat flux Q_i at say t_o is used to update the value of temperature at a time: $t_o + \Delta t$. This is done repeatedly to obtain the profile of given interval n over a given time period from say t_o to t_1. Solving for temperature we find

$$T(n,K,t_o+\Delta t) = T(n,K,t_o) + \left[\frac{\Delta t}{[P(K)][CM(K)][\Delta Z(K)]}\right]\left[\sum_{i=1}^{N} Q_{oi}(t_o) + Q_T\right] \qquad (3)$$

where $T(n,K,t_o+\Delta t)$ is the updated temperature. When considering the surface volume the updated temperature of the surface is:

$$T_o(t_o+\Delta t) = T(t_o) + \left[\frac{\Delta t}{[P(1)][CM(1)][\Delta Z(1)]}\right]\left[\sum_{i=1}^{6} Q_{oi}(t) + Q_T\right] \qquad (4)$$

Note that N=6 represents the six basic heat transfer mechanisms mentioned earlier.

Five of the six mechanisms depend on the temperature at the surface and the temperature of the atmosphere. However, conduction depends on value of the temperature at the surface and the temperature of the first interval below the surface layer. This is stated as

$$Q_{o1} = -AK(1)\left[\frac{T(1,1) - T(2,1)}{[\Delta Z(1) + \Delta Z(2)]/2}\right] \qquad (5)$$

AK(1) - Conductivity of layer 1

where:

T(1,1) = surface temperature.

T(2,1) = temperature of first interval in second layer.

Distance are taken between the midpoints of each interval.

Hence the temperature T(2,1) must be known at a time t_o to compute Q_{o2} for use in the update of T_o as given in Equation 4. The value of T(2,1) must also be updated since it depends on the temperature difference of adjacent intervals (surface layer and T_{22}). It also follows that all intervals must be updated during any particular time interval Δt.

At intervals that do not constitue air/surface boundaries, the only method of heat flow is conduction. Hence for updating temperature intervals between boundaries, N=1; and since conduction is the only heat flow mechanism we have from Equation 3,

$$T(n,K,t_o+\Delta t) = T(n,K,t_o) + \left[\frac{\Delta t}{[P(K)][CM(K)][\Delta Z(K)]}\right] Q_{o1}(K,t_o) \qquad (6)$$

where:

$Q_{o1}(K,t_o)$ is taken as net conduction thru interval k at time t_o;

hence

$$Q_{o1}(K,t_o) = AK(K)\left[\frac{T(n-1,K) - T(n,K)}{\Delta Z(K)} - \frac{T(n,K) - T(n+1,K)}{\Delta Z(K)}\right] \qquad (7)$$

Positive direction is taken as heat flow into volume interval. Combining Equations 6 and 7 we have:

$$T(n,K,t_o+\Delta t) = T(n,K,t_o) + \left[\frac{(\Delta t)AK(K)}{[P(K)][CM(L)]}\right]\left[\frac{T(n-1,K)-2T(m,K,t_o)+T(n+1,K)}{\Delta Z(K)^2}\right] \quad (8)$$

Equation 8 may be seen as Equation 5 rewritten in finite differential form and with terms rearranged to solve for the temperature at time $t_o + \Delta t$. For all features the number of layers is not limited. However, six layers are usually sufficient.

For features where one boundary is coincident with the surface of the Earth (roads, etc) a lower boundary is assumed at about 1-meter distance from the surface. Within this distance, the volume may be partitioned into layers and intervals as is appropriate to physical constituency. At the lower boundary or the last interval in the bottom layer the temperature is assumed to be constant. If the feature is elevated then both the upper and lower boundaries are assumed to be in contact with the air and the same mechanisms are operating on each surface layer.

2. SPECIFIC FORMULATIONS

a. Conduction - Surface Heat

Conduction for heat flow away from a surface volume is given in Equation 5. Conductivity through a surface layer depends strictly on the temperature gradient between the surface layer and the first interval below it.

b. Solar Energy Input

Here we are concerned with total combined direct and diffuse solar energy at the surface. Consideration is given to the ability of the surface to absorb solar energy. Also considered is obscuration by ground vegetation and surrounding vegetation canopy. The equation for heat flow taken from Reference 1 is given as

$$Q_{o2} = A_s(1-OB)P(0)^{(1+C^2\tan^2\theta)^{1/2}} \quad (9)$$

where:

A_s = fraction of solar energy reaching surface that is actually absorbed by the surface $0 \leq A_s \leq 1$

OB = Fraction of ground covered by vegetation $0 \leq OB \leq 1$

S(t) = Total direct and diffuse solar energy

P(0) = Probability of clear line-of-sight at Zenith thru overhead canopy $0 \leq P(0) \leq 1$

C = Canopy characteristic factor

θ = Angle of sun from Zenith

The expression $P(0)^{(1+C^2\tan^2\theta)^{1/2}}$ relates to the probability of solar penetration thru overhead canopy as a function of the zenith angle θ. The value of P(0) is a measure of probability of an unobscured line-of-sight when the zenith angle is zero. The value of C is a measure of foliage density which is a function of leaf and branch distribution and size.

These parameters have an intuitive character which it would seem could only be grossly related to actual physical configuration. For no overhead canopy P(0) = 1 and C = 0; whereas in the case very dense foliage C could take on values in the range from 50 to 100. From this expression, the penetration probability for dense foliage ($50 \leq C \leq 100$) drops very quickly at angles away from Zenith but drops more slowly for sparse covering ($0 \leq C < 1$).

Rather than rely strictly on gross or intuitive estimates it might be possible to calculate values for C if P(0) could be measured or calculated for several values of θ. The value for C from above is calculated from:

$$C = \frac{1}{\tan\theta}\left[\left[\frac{\ln P(\theta)}{\ln P(0)}\right]^2 - 1\right]^{1/2} \qquad (10)$$

In Reference 7 a theoretical formulation is suggested to relate penetration probability to leaf distribution, area coverage over ground and orientation distribution of leaf surfaces. From this formulation a penetration probability was calculated as a function of θ. An example of a set of these calculations taken from Reference 7 is given in Table 1:

TABLE 1

PROBABILITY OF LIGHT TRANSMISSION
VERSUS ZENITH ANGLE - REFERENCE 7

P(θ)	θ
.63	5°
.63	15°
.63	25°
.63	35°
.62	45°
.61	55°
.57	65°
.47	75°
.13	85°

Referring to Equation 10, a value of C = .32 was calculated and P(0) from Table 1 was assumed to be .63. This value of C was used, in turn, to calculate from Equation 9; values for P(θ). The results are as shown in Table 2:

TABLE 2

PROBABILITY OF LIGHT TRANSMISSION VERSUS
ZENITH ANGLE CALCULATED FROM EQUATION 9

P(θ)	θ
.629	5°
.629	15°
.626	25°
.623	35°
.615	45°
.60	55°
.57	65°
.49	75°
.17	85°
0	90°

Alternate expressions such as given in Reference 7 might be used to obtain more exact calculations for $P(\theta)$. However, this would depend on availability of data regarding leaf size, distribution, orientation and dispersion for reasonable results. The expression as given in Equation 9 still seems to be reasonable, however, since variability and complexity of arrangement of vegetation components may preclude calculations from detail consideration of the above parameters.

In the foregoing paragraph, a value of P(0) equal to .63 and a C equal to .32 was shown to give a value of $P(\theta)$ consistent with values computed from more exact knowledge of world conditions. In this model a value of P(0) equal to .8 was used and C was assumed to equal .3 as suggested in Reference 1.

c. Net Radiation Transfer

The net radiation transfer is based upon the difference between energy lost due to radiation and that absorbed from surrounding atmosphere. Here broadband greybody radiation is assumed in the energy exchange which was considered reasonable for the types of surfaces and materials involved. The equation used is:

$$Q_{o3} = (-\sigma\varepsilon_o T_o^4 + \sigma\varepsilon_A \alpha_A T_A^4) \; [1 - (U)\, CC(t)] \qquad (11)$$

where:

σ = Stephan Baltzman Constant
ε = thermal emissivity of surface
T_o = Surface Temperature - degrees Kelvin
T_A = Air Temperature - degrees Kelvin
U = Cloud type coefficient
CC(t) = Cloud cover - Percent
ε_A = Emissivity of atmosphere
α_A = Absorption (Long wavelength) of surface

The U factor refers to cloud density and is considered variable from .9 for thick low clouds to .2 for thin high-altitude clouds. The factor CC(t) is the percentage of clear hemisphere that is covered with clouds.

Note from the term in the second set of parentheses that conditions of clear sky or thin clouds gives high radiation exchange as contrasted to overcast conditions where radiation exchange would be considerably reduced.

The emissivity of the atmosphere can be determined from the following formulation taken from Reference 1.

$$\varepsilon_A = a + b\left[[RH(t)][P_s(T_a)]\right]^{1/2} \tag{12}$$

where:

$RH(t)$ = Time varying relative humidity

$P_s(T_a)$ = Saturation vapor pressure of atmosphere at atmospheric temperature T_a

a = .53

b = .047

In some literature, variations to the above formulation for ε_A were found that give a slightly larger value for ε_A. However, Equation 12 was used by ERIM as part of their target temperature modeling and validation program (Reference 1). Therefore, it's use seems appropriate in this effort.

d. Convection Transfer

The heat loss or gain due to convection is one of the most significant heat exchange mechanisms and can vary considerably depending on the wind conditions near the surface. Both free and forced convection can be factors in the molecular diffusion of heat. The rate of transfer depends on a temperature gradient between surface and atmosphere over an arbitrary vertical distance from the surface and is also a function of a surface roughness parameter. The surface roughness can be considered as the average variations or deviation in thickness of the surface layer.

The expression for heat transfer due to convection may be given as

$$Q_{o4} = C_V + C_p P K_h \frac{\Delta T}{\Delta Z} \tag{13}$$

where:

C_V = Transfer due to free convection
C_P = Specific heat of air
P = Air Density
T = Temperature gradient over some distance Z above the surface
K_h = Heat diffusion coefficient

From Reference 3 an expression for K_h was derived, assuming wind velocity and air temperature are measured at 160 centimenters above the surface. This assumption is consistent with available measured input data.

$$K_h = \frac{(.05)(160/Z_o)^{\beta}(Z_o)\ V_M(t)\ (2682)}{\ln(160/Z_o)} \qquad (14)$$

If free convection is considered small in relation to forced convection or if one assumes that some wind conditions always exist, it can be argued that only force convection need be considered. Combining Equations 13 and 14 and noting that the ΔZ term in Equation 14 is equivalent to 160 cm, we have

$$Q_{o4} = \frac{(.05)(C_P P)(160/Z_o)^{\beta}\ V_M(t)\ (2682)(T_o - T_A)}{(160/Z_o)(\ln\ 160/Z_o)} \qquad (15)$$

where:

Z_o = surface roughness in C_m
$V_M(t)$ = wind velocity expressed in MPH
β = stability coefficient

$$\beta = \begin{cases} 1 + .000672\ (T_o - T_A) \text{ for } T_o > T_a \text{ - unstable conditions} \\ 1 + .00639\ (T_o - T_A) \text{ for } T_o \leq T_a \text{ - stable conditions} \end{cases}$$

The above formulation given by Equation 15 was used in this program to calculate convection heat transfer from rough surfaces where turbulent conditions exist at the air/surface boundary.

e. Rain Heating Or Cooling

The effect of rainfall on the surface is treated thru direct heat exchange between the rain and surface volume. The penetration/runoff problem is not treated in the current model. This would require that the percent moisture contained in the surface volume be considered. For this model the heat exchange is a function of the temperature difference between the surface and rain during a particular time increment. The expression is

$$Q_{05} = (RI)(PW)(CW)(T_O - T_R) \qquad (16)$$

where:

RI = Rainfall rate
PW = Density of water
CW = Specific heat of water
T_R = Rain temperature
T_O = Surface temperature

f. Water Evaporation Loss

The transfer of water from the surface to the adjacent atmosphere is a process taking place thru a turbulent exchange. The rate of transfer of water vapor is a function of vapor pressure differential between the surface and air and the amount of wind velocity. The heat lost is then the latent heat of vaporization multiplied by this transfer rate. This is expressed as:

$$Q_{06} = \frac{(L)(k_c)^2 V_M(t)(2682)}{\ln(160/Z_o)^2 (R)(T_A)} \quad (.622\left[P_s(T_o) - RH(t) - P_s(T_A)\right]) \qquad (17)$$

where:

L = Latent heat of vaporization
k_c = Von Karmen's constant = .4
$V_M(t)$ = Wind velocity - .MPH
Z_o = Surface roughness
R = Rankine constant
$P_s(T_o)$ = Saturated vapor pressure of water at surface temperature
$P_s(T_A)$ = Saturated vapor pressure of water at air temperature
RH(t) = Relative humidity

3. ELEVATED TARGET

The foregoing discussion applies to heat transfer convections at the upper air/surface boundary. This would then apply to features listed under category A. However, lower boundary conditions can be different, depending on the elevation of the target. In the case of a road (non-elevated), we have multiple layers extending from the surface to a depth of about 1 meter. At this depth, a more constant temperature can be assumed for a lower boundary condition. If the bottom surface is elevated then it is subject to heat transfer effects similar to those of the top surface. In the case of an elevated surface there could be an independant heat source below, the surface contributing to the total energy flux change with either the air or ground below the bottom surface. Two heat transfer effects; namely solar irradiation and thermal radiation exchange, require special consideration.

The portion of solar irradiation on the bottom surface is the amount reflected from the ground surface. This is expressed as

$$Q_{o2B} = (1 - A_s)Q_{o2} \tag{18}$$

where terms are defined previously (see Equation 9).

The radiation exchange may be expressed as

$$Q_{o3BA} = -\sigma\ \varepsilon_o * T_o^4 - \alpha_T \varepsilon_A T_A^4 + \alpha_T Q_T \tag{19}$$

where:

α_T = Long wavelength surface absorption
Q_T = Independent non-solar energy source

The factor $\varepsilon_A T_A^4$ would be replaced by a radiation term from ground, water etc. if exchange is assumed to take place directly with these features. This factor would be: $\sigma\varepsilon_s T_s^4$ where ε_s = emissivity of surface, T_s = absolute temperature of surface.

4. THIN ACTIVE TARGET

For the case of a target vehicle the surfaces are assumed to be thin, which means that they are modeled as only one layer and one interval. External to vehicle the processes of radiation, solar irradiation evaporation, etc. are operating as with other types of targets. However, for the case of a truck or jeep the engine can be modeled as a heat source irradiating from under the hood. The energy from the engine has been measured. The data and discussion are contained in Reference 1.

The radiation exchange is given by

$$Q_{o3THI} = (-\sigma(\varepsilon_o \quad T_o^4 - \alpha_T \varepsilon_A T_A^4) + \alpha_T Q_T)\,[1-(U)(CC(t)] \qquad (20)$$

For the heat transfer by convection the problem becomes more difficult since wind or turbulent flow aorund a three-dimensional irregular object is quite complex.

The hood is represented as a flat plate. On this basis a heat transfer coefficient may be calculated based upon laminar flow over the surface. This gives a heat transfer coefficient as a function of the wind velocity and length of hood. A heat transfer coefficient was calculated and used in surface temperature prediction.

However, a formulation contained in Reference 5 gave more reasonable results and was used to calculate vehicle hood temperature shown in Figures 9 and 13. This is given as

$$h = 1.7|T_o - T_a|^{1/3} + \frac{(6)[1.32V_M(t)]^{0.8}}{(LHO \cdot 10^{-2})^{0.2}} \qquad (21)$$

where:

h = Heat transfer coefficient for hood
LHO = Length of vehicle hood
VM(t) = Wind Velocity - MPH

The transfer by convection is then given by

$$Q_{o4s} = h(T_o - T_A) \tag{22}$$

where

Q_{o4s} = Heat energy transfer by connection from smooth surface

5. SHADOW

Thermal shadows are usually made by parked vehicles which obscure a significant portion of the solar radiation falling on fully illuminated surfaces. The study of these thermal shadows which are visible to the infrared system can be instructive from a tactical standpoint if details about previous vehicle activity can be accurately inferred. The shadow signature depends on the length of time that the vehicle was parked, specific time period when the vehicle was in place, and the length of time since departure.

Prediction of thermal signature requires that temperature of the surface obscured by the vehicle be predicted. The temperature difference between a shadowed area and the illuminated region during vehicle obscuration and after vehicle removal is a measure of the contrast difference and an indication of the number of hours during which the shadow could be detectable.

As in Reference 1, solar illumination in a shadowed area is assumed to be reduced by 1/5 the value in an illuminated area, so:

$$Q_{o2s} = \frac{Q_{o2}}{5} \tag{23}$$

Furthermore, the bottom of the vehicle is assumed to radiate as a black body exchanging energy with the surface below it. Then we have:

$$Q_{o3s} = \sigma(-T_s^4 + \varepsilon_o * T_o^4) \tag{24}$$

The wind velocity is assumed to be zero under the vehicle so that during a dry season with no precipitation only conduction, radiation or solar irradiation control the temperature of the shadowed surface when the surface is obscured by a vehicle.

6. VEGETATION THERMAL MODEL

a. General Considerations

Vegetation is an important part of the scenario because it forms, in most cases, a large portion of the background in an infrared scene.

The signature patterns from the vegetation are manifested in this radiation from a complex of surfaces constituting outer tree foliage, bushes, scrub growth, grass, etc.

The size, shape, relative orientation and density of vegetative surfaces can vary considerably over a given scenario and the problem of predicting radiation values seem unduly complex. However, the same heat transfer mechanisms operate on each constituent be it a leaf, blade of grass, pine needle, etc. These mechanisms have been studied, and measurements and formulations for quantifying heat flux rates have been made for the individual vegetation component.

Interaction between components or temperature dependency of a given region of vegetation or surrounding bio-mass is also important (see Reference 7). This is a separate consideration and could add considerable complexity to model, as interactive effects could be as variable as size, arrangements, etc. of vegetative elements themselves.

Therefore, in this model, energy exchange is based upon that which occurs in the individual leaf, blade of grass, etc. and a temperature profile can then be calculated over a given time period.

Four basic heat exchange mechanisms operate on the leaf. These are (1) solar irradiation, (2) radiation exchange with the atmosphere, (3) convection, and (4) transpiration. The leaf furthermore has the ability to regulate its temperature thru its stomata which controls water vapor and gaseous exchange with the atmosphere. The stomata can vary considerably in terms of size, distribution and depth of openings, all of which affect internal diffusion resistance to gas or water vapor exchange.

From the above considerations, smaller leaves are more susceptible to windspeed variation and changes in transpiration but larger leaves are effected to a greater extent by changes in solar radiation.

In certain large leaves, for example, stomation is reduced as compared to their smaller companions. These large leaves then thrive in shady moist areas where reduced solar energy and increased moisture availability are more favorable to survival. Smaller leaves with increased stomation, better heat dissipation capability and less sensitivity to solar insolation thrive nicely in dry areas with high solar irradiation.

Sensitivity to solar radiation can result in an increased warming effect on large leaves and can also cause large leaves to be relatively cool. For example, dew can be more likely to form on the larger leaves during cool morning hours. These same leaves can also seem warm to "touch" at other periods of the day.

As mentioned earlier the leaf can assume a variety of orientations and can in fact change orientation to remain normal to solar radiation. For this modeling effort a horizontal leaf orientation is assumed to simplify modeling, yet remain somewhat consistent with actual real-world conditions.

Figure 6 illustrates the heat exchange process:

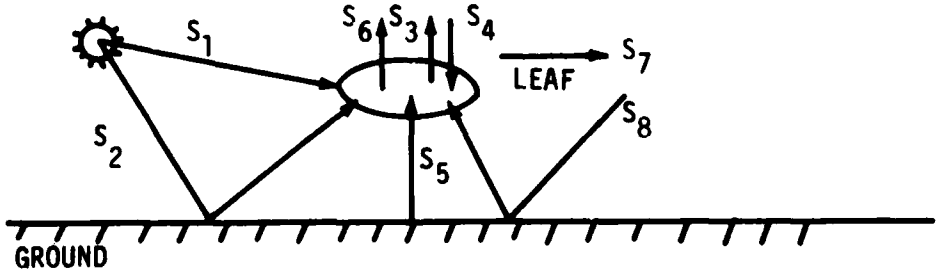

Figure 6. Heat Exchange - Leaf

where:

S_1 = Direct and Diffuse radiation from sum
S_2 = Ground reflected direct and diffuse radiation
S_3 = Leaf radiation to external environment

S_4 = Absorbed along wavelength radiation from atmosphere
S_5 = Long wave length radiation from the ground
S_6 = Leaf transpiration loss
S_7 = Heat transfer due to convection
S_8 = Ground reflected atmospheric long wavelength radiation

The foregoing heat transfer components can be combined into four heat-exchange terms covering solar irradiation, radiative, convective and transpiration effects.

The leaf represents a small mass and it can be assumed that steady-state conditions prevailed shortly after any change input variables (solar energy, wind, etc). Therefore the heat balance is

$$\sum_{i=1}^{4} Q_i = 0 \tag{25}$$

where Q_i is the heat flux rate of i^{th} heat component into or out of leaf surface.

b. Solar Irradiation

The solar irradiation on leaf may be expressed as

$$S_1 = \alpha_{SL} S(t) + \alpha_{SL}(1-A_s)\, S(t) = \alpha_{SL} S(t)(2-A_s) \tag{26}$$

where:

α_{SL} = Short wavelength absorption of leaf
A_s = Short wavelength absorption of ground
$S(t)$ = Direct and diffuse solar energy

The first term Q_1 was found by combining the value in S_1 above with S_5.

$$S_5 = \varepsilon_o \sigma T_o^4 \tag{27}$$

which is long wavelength radiation from ground,
so that

$$Q_1 = \alpha_{SL} S(t)(2-A_s) + \alpha_L \varepsilon_o \sigma T_o^4 \tag{28}$$

where:

α_L = long wavelength absorption of leaf.

c. Radiative Transfer

The radiation from the leaf may be expressed simply as the difference between S_3 and S_4 or

$$Q_2 = - \sigma\varepsilon_L T_L^4 + \sigma\varepsilon_A \alpha_T T_A^4 \tag{29}$$

where:

ε_L = Leaf emissivity
σ = Stephen Baltzman constant
ε_A = Atmospheric emissivity obtained from Equation 13

d. Convection

The energy exchange due to convection depends on wind velocity, leaf size and temperature difference between the leaf and the surrounding atmosphere.

This is given as:

$$Q_3 = -h_L(T_L - T_A) \tag{30}$$

where:

h_L = Convection heat transfer coefficient

Various expressions for h_L can be found in the literature (References 1,6) which permit calculation of free or forced convection. Sufficient wind velocity was assumed to exist always, so that forced convection is dominant. The follow expression was employed in the model.

$$h_L = C\left[\frac{V_M(t)(2682)}{XPR}\right]^{1/2} \tag{31}$$

where:

XPR = Leaf width
C = Form factor which depends on leaf

From data given in Reference 4 a value of 10^{-3} was computed for C.

e. Transpiration

This accounts for heat loss due to latent heat of evaporation of water from the leaf surface. The rate of heat flow depends on the vapor pressure gradient between the leaf and air and is inversely proportional to total leaf resistance to vapor transfer. The total leaf resistance is composed of boundary layer resistance and internal diffusion resistance. Reference 6 discusses calculation of internal diffusion resistance. The expression is given as:

$$Q_4 = \frac{C_p P[P_S(T_L) - R_H(t)P_S(T_A)]}{a(R_{BL} + R_G)} \qquad (32)$$

where:

R_G = Internal diffusion resistance
R_{BL} = Boundary layer resistance
a = Constant = .55 millibars

Other terms as defined previously (see Equation 17).

SECTION IV

MODEL IMPLEMENTATION AND ANALYSIS OF PRELIMINARY RESULTS

The foregoing model was implemented and various computer runs were made to test the reasonableness of formulations and assumptions.

Input data for the model were taken largely from Reference 1. The temperature profiles for a dirt road, soil, hood of truck (engine on and engine off), vegetation, and a bridge were computed. This permitted exercising most of the options contained in the model. The temperature profiles for dirt road and soil were computed using Equation 4 for surface temperature together with Equations 5, 9, 11, 12, 13, 14, and 15 for the energy fluxes. Equation 8 was used to update temperature below surface. For the vehicle hood Equation 4 was used together with Equations 9, 12, 20, 21, and 22 for energy flux. Vegetation curves were calculated using Equation 25 together with Equations 26 - 32 for energy flux.

Two sets of time varying input data were employed for S(t), RH(t), VM(t), CC(t), and $T_A(t)$. This is shown in Figures 7 and 8. The first set is typical summer data and the second set is based upon measured data for a summer season.

The wood and soil are similar in physical configuration in that they represent high thermal inertia features. The following parameters shown in Table 3 were employed for the wood and soil. All units were as specified earlier.

For the hood of the vehicle, the following parameters in Table 4 were used.

Note that for dirt, wood, and soil, a surface layer thickness of 1 centimeter was assumed. Ten intervals were used to subdivide the two layers below the surface layer. The active target was modeled as a single layer of metal of 0.3 centimeter in thickness. The bridge was assumed to be solid concrete of 45 centimeters in total thickness, and a 1-centimeter thick surface layer was assumed for both the upper and lower surface layer. The total list of parameters is given in Table 5.

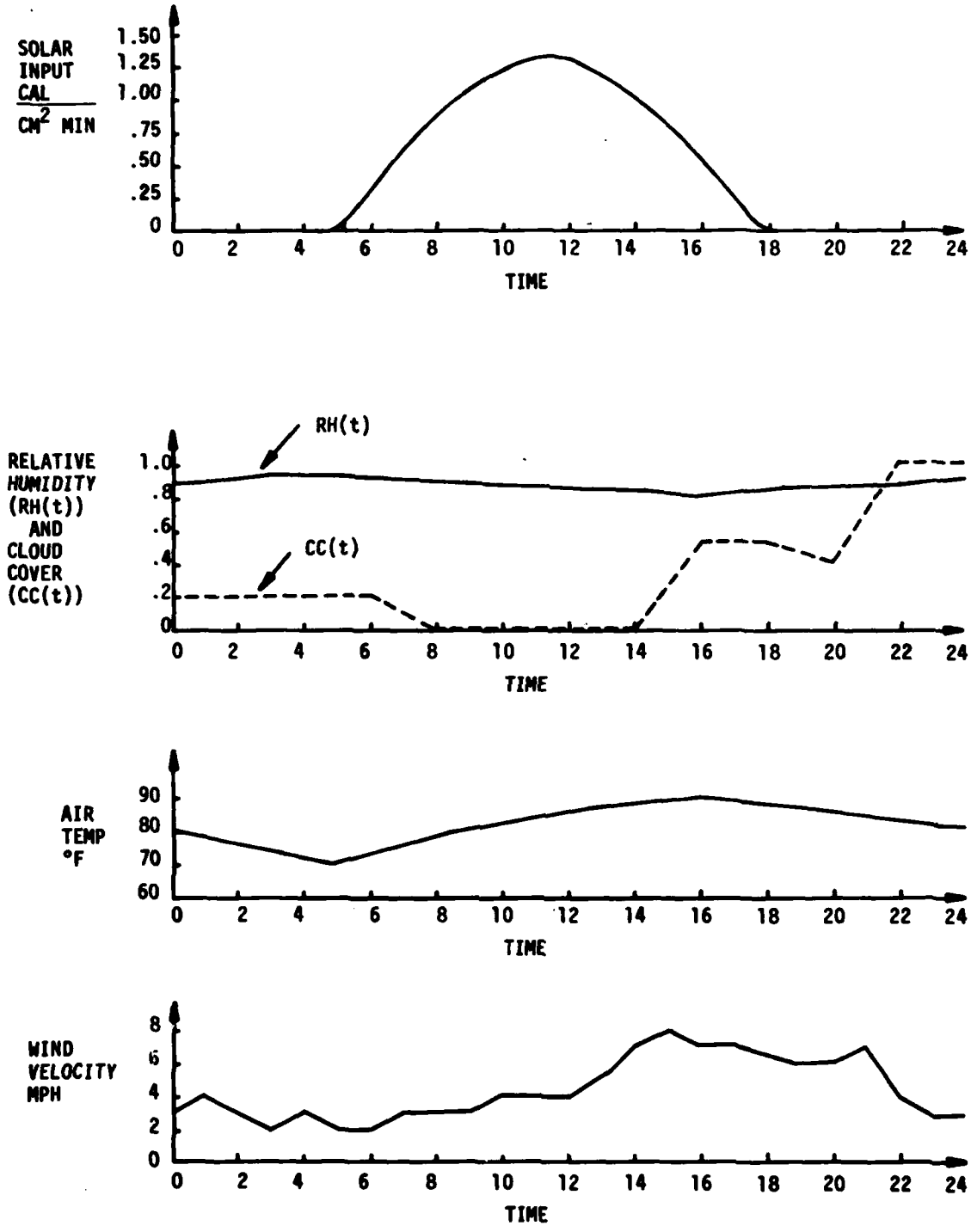

Figure 7. Typical Summer Data

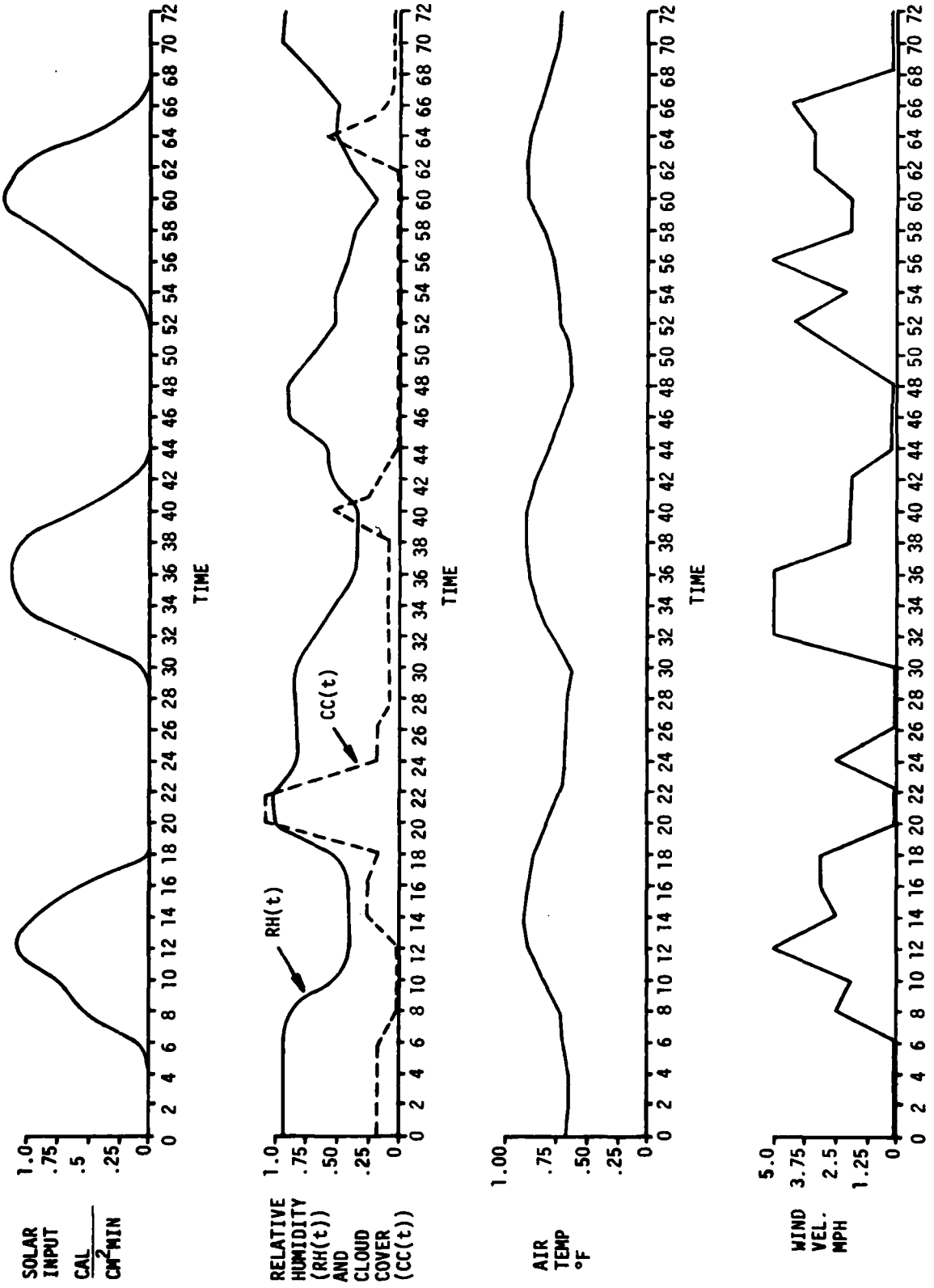

Figure 8. Real Summer - Environmental Data

TABLE 3

ROAD AND SOIL PARAMETER VALUES

	Road	Soil
NLAY	3	3
LAYER (K)	1, 10, 10	1, 10, 10
AK(K)	.233, .233, .33	.116, .116, .17
D(K)	.416, .416, .416	.286, .286, .338
ATH(K)	2, 1.9, 11	1, 2.9, 9
Zo	.2	.5
A_s	.8	.8
OB	0	.5
C	.3	.3
ε_o	.9	.96
U	.8	.8
Po	.8	.8
RI	0	0
PW	-	-
CW	-	-
DAY	196	196
ALAT	40°N	40°N
T_R	-	-
DELT	1 minute	1 minute

TABLE 4

VEHICLE HOOD PARAMETER VALUES

NLAY -1

AK(K) - 6.45

D(K) - 7.33

ATH(K) - .3

Zo - Not applicable to smooth target

AL_S - .95

OB - 0

C - .3

ε_o - .95

U - .8

Po - .8

RI - 0

PW - Not required

CW - Not required

DAY - 196

ALAT - 40°N

T_R - Not required

DELT - 1 minute

Q_T - .5 $\frac{CAL}{CM^2\text{-}MIN}$

LHO - 150

TABLE 5

BRIDGE - PARAMETER VALUES

NLAY - 3

LAYER(K) - 1, 10, 1

AK(K) - .3, .3, .3

D(K) - .5, .5, .5

ATH(K) - 1, 4.3, 1

Zo - 1

A_s - .7

OB - 0

C - .3

ε_o - .95

U - .8

Po - .8

RI - 0

PW - Not used

CW - Not used

DAY - 196

ALAT - 40°N

T_R - Not used

DELT - 1 minute

The time increment of 1 minute resulted in a convergence of the solution and reasonable temperature profiles for the above features. Increasing the number of intervals beyond 10 in layers below the surface layer did not seem to affect the results appreciably. But a ratio of time increment Δt to interval thickness TH(K) that was less than or equal to 1 resulted in convergence of solution to a reasonable set of temperature values. Apparently, larger time increments might be selected with a corresponding increase in interval thickness if desired. Of course, the tradeoff here is the accuracy of the temperature calculations.

The curves shown in Figure 9 using data from Figure 7 and Tables 3 and 4 represent temperature profiles for dirt road, soil and active target.

The active target with correspondingly low thermal inertia and high conductivity shows wider temperature excursions than that for the soil and and dirt road.

The values assumed for initial conditions do not seem critical since, as shown, stability is reached within the first 24 hours. The data was repeated over 24-hour intervals so convergence or constancy of total temperature differentials during each day were readily observable.

Typical summer temperature profiles for vegetation and bridge are shown in Figures 10 and 11, respectively. Typical summer shadow curves are shown in Figure 12.

The temperature profiles in Figure 13 are particularly interesting. Several things are noted and correlatable to Figure 8 input data;

1) Time of sunrise and sunset occurring at about 5 AM and 7 PM respectively are noted.

2) From curve 3 note that thermal crossover of hood temperature with respect to soil or road occurs regularly at about sunrise and just after sunset. This is consistent with observation of real-world thermal imagery.

3) The time of maximum temperature corresponds to the time of maximum air temperature rather than maximum in solar irradiance. During the period from 6 AM to 8 AM, note a sudden leveling of temperature rise on curve 4. At this time cloud cover drops and wind velocity increases.

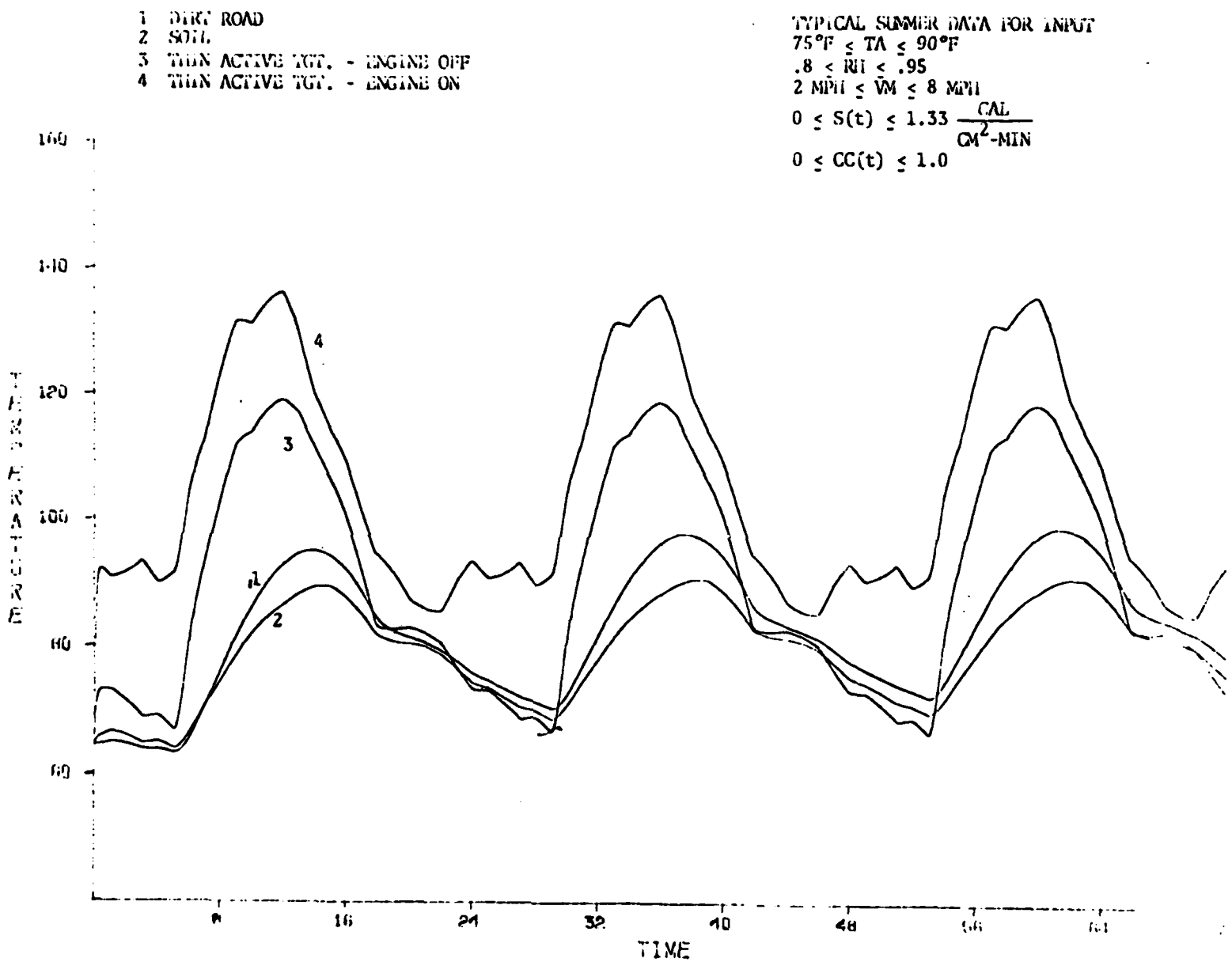

Figure 9. Temperature Profiles - Typical Summer Data

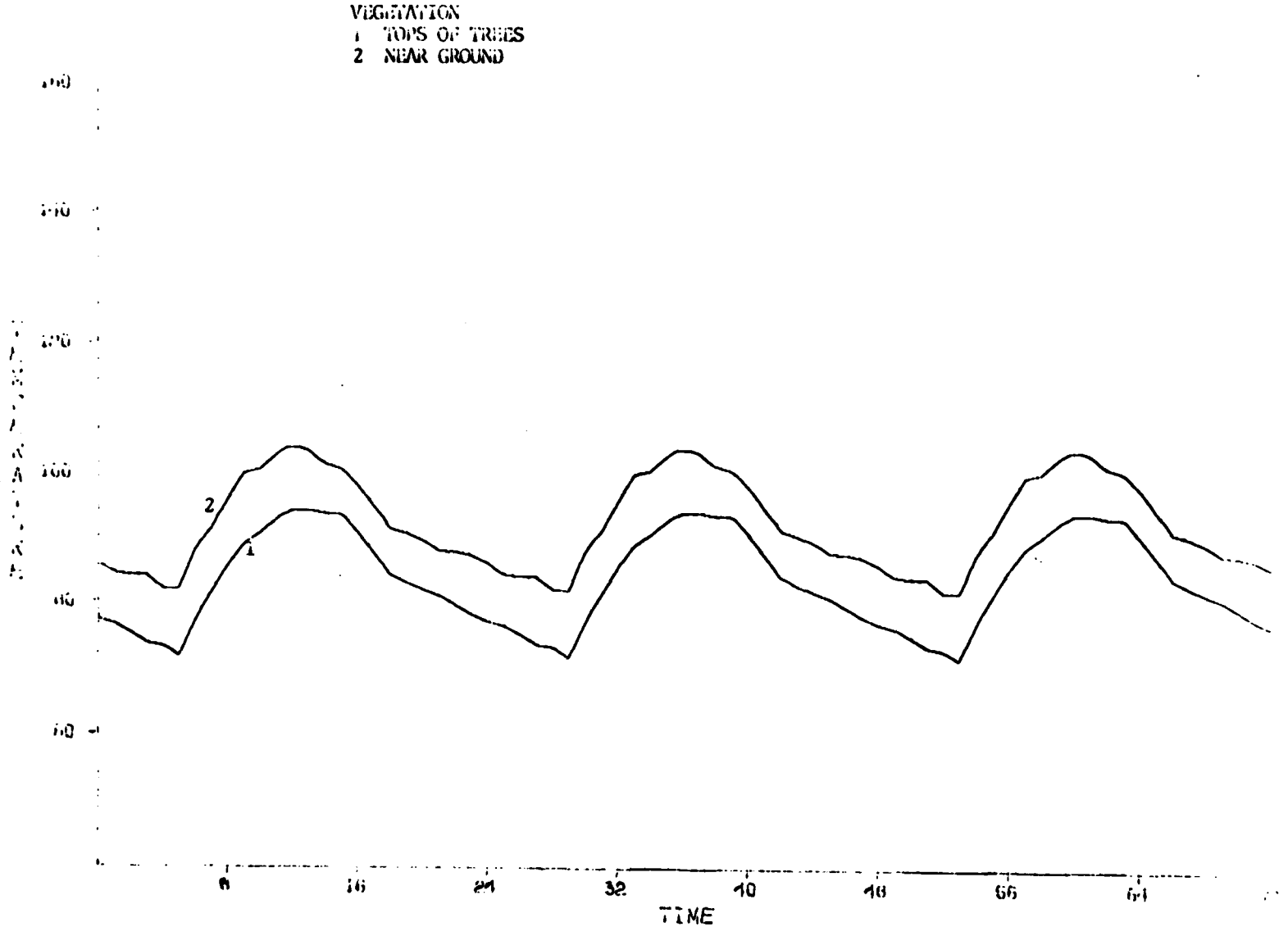

Figure 10. Temperature Profile for Vegetation - Typical Summer Data

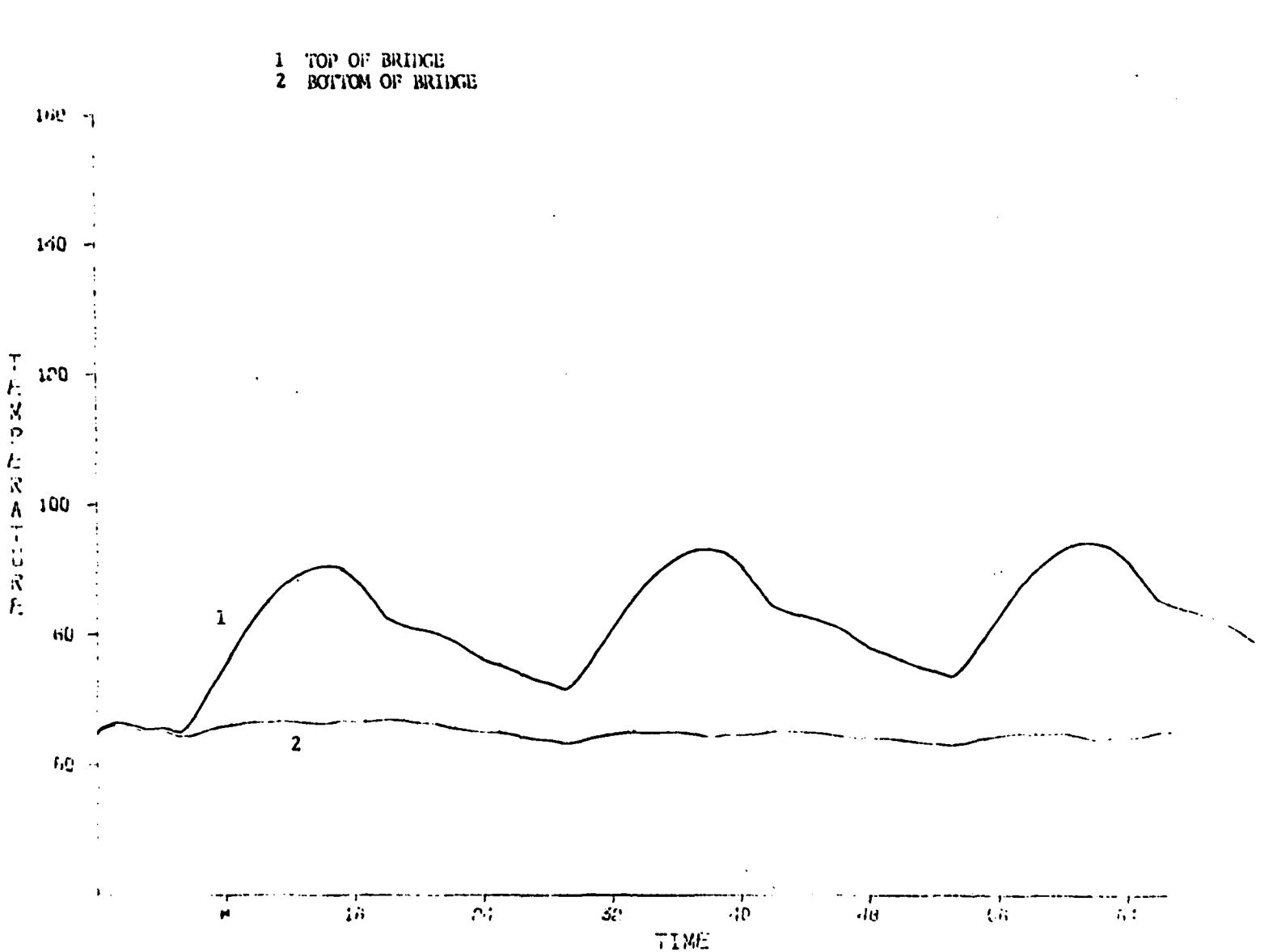

Figure 11. Temperature Profile for Concrete Bridge - Typical Summer Data

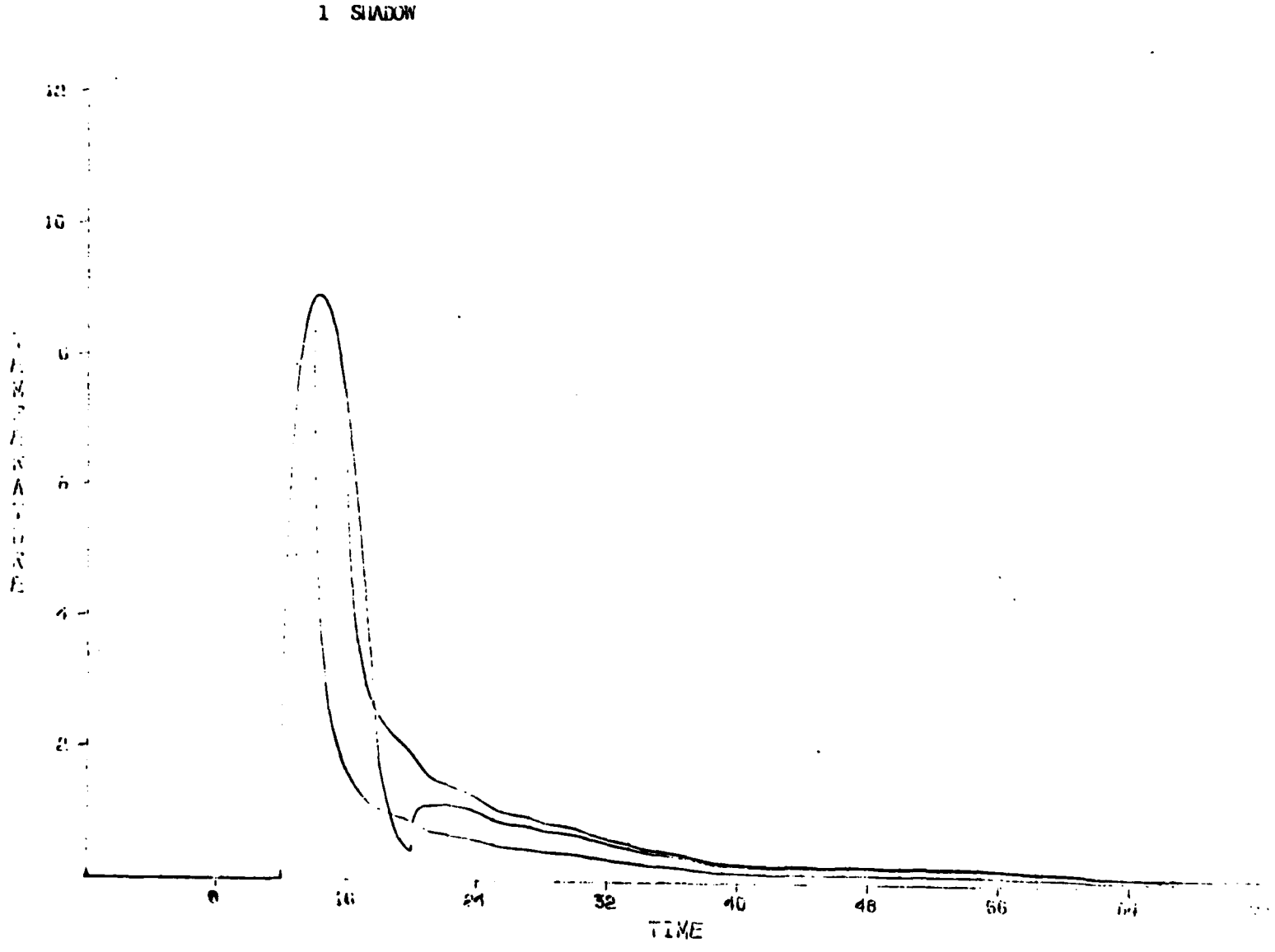

Figure 12. Shadow Curves - Typical Summer Conditions

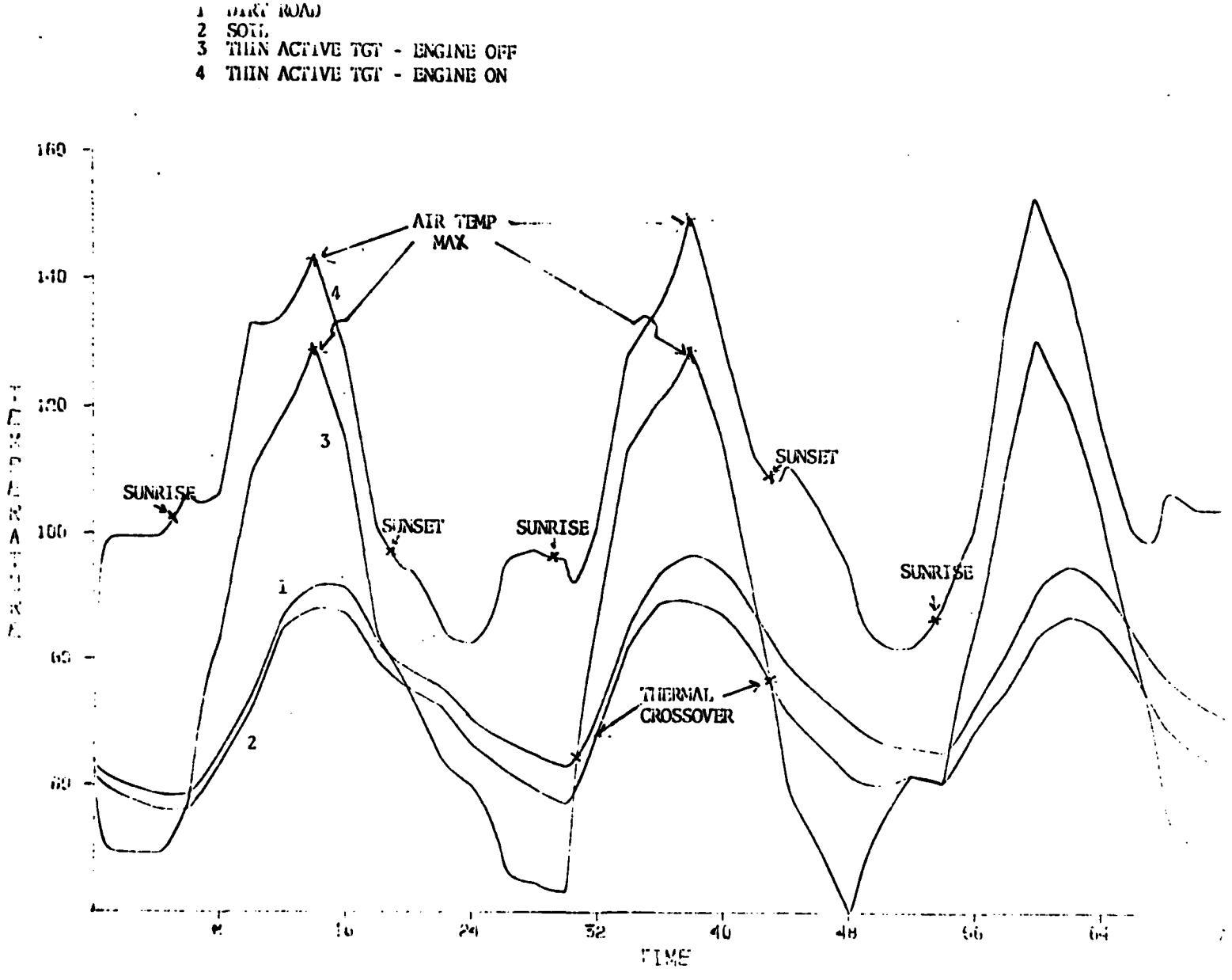

Figure 13. Temperature Profiles - Real Summer Environmental Data

Since T_L is much above air temperature the increase in radiation and convection loss causes a significant effect. On curve 3 we are closer to air temperature and no dramatic effect is noted and temperature continues to rise as solar insolation increases.

4) Consider the period from sunset to sunrise at the end of first 24 hour period. During the first half of this period from 7 PM to midnight, solar energy is zero, air temperature is dropping and wind velocity is still sufficient to permit cooling of the hood surface. This cooling is of course more rapid when the engine is not operating.

5) During the second half of the period from 12 PM to 5 AM wind velocity decreases and cloud cover has dropped appreciably from the first half of the evening. Note that with the engine off the reduced wind velocity decreases the convection transfer since T. < Ta and the radiation loss increases with low cloud cover, causing the surface to cool appreciably.

6) However, with the engine running (curve 4) the radiation from the hood reduces the effect of losses due to the drop in cloud cover. In this case T_L > Ta and the reduction in wind velocity as seen from Figure 8 reduces the losses and results in an actual temperature increase during this time.

7) Consider the sunset to sunrise period of the next day and note that the cloud cover is essentially zero which maximizes the radiation loss.

8) From 12 PM to 5 AM, the wind velocity increases and in the engine off condition, T_L < Ta and warming occurs.

9) The vegetation profiles of Figure 14 contain sharp temperature changes which are not surprising since the leaf component is a small thermal loss and capable of reacting quickly to input variable changes.

a) We note that the peak vegetation temperature corresponds to the peaks in air temperature.

b) Refer to curve 2, note the sharp rise in temperature starting at 4 AM followed by a quick drop around 6 AM to 8 AM. As determined from Figure 8, wind velocity increases at 6 AM, and since $T_L > T_a$ a sharp temperature decrease occurs. On curve 3 where T_L is close to T_a the change is not apparent.

c) During the time period from 2200 HRS to 0200 HRS (10 PM - 2 AM) first day the wind velocity increases from .1 to 2.5 MPH and then drops back to .1 MPH. Comparing temperature responses in curve 2 and 1 during

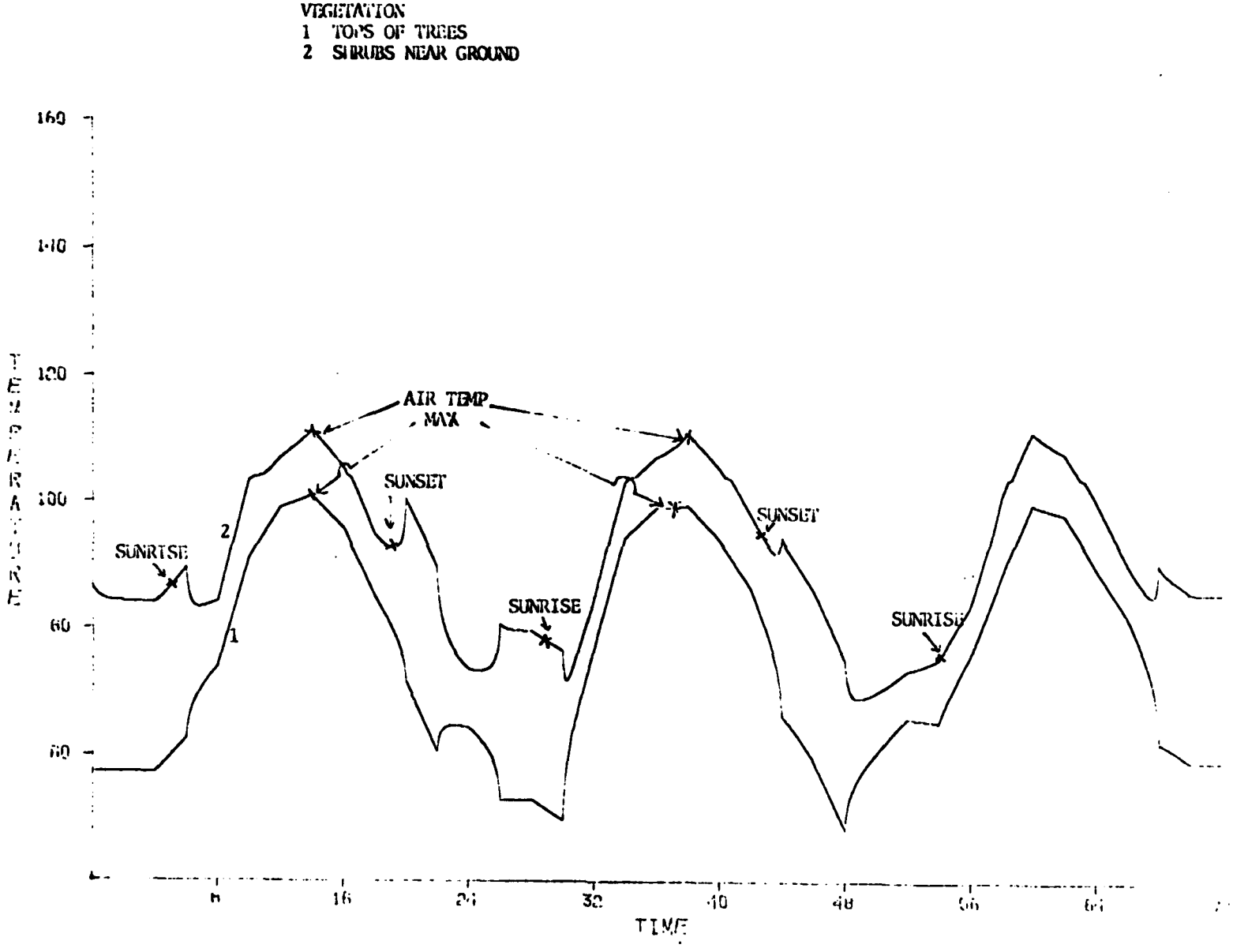

Figure 14. Temperature Profile for Vegetation - Real Summer Environmental Data

the first 2 HRS when wind velocity is increasing we see that for curve 2, $T_L > T_a$ and cooling occurs; whereas for curve 1, $T_L < T_a$ and a slight warming occurs. The reverse happens in time during the second half of the period when the wind velocity is decreasing.

d) On curve 1, after 48 HRS a warming effect is seen since wind velocity decreases and $T_L < T_a$.

Figure 15 is a real-summer temperature profile for a bridge.

e) The curves representing shadows profiles are shown in Figure 16. The vehicle was parked at 1200 HRS the first day and left in place for 2, 4, 8 hours. Note the temperature difference for each case measured from 1400, 1600, and 2000 hours respectively.

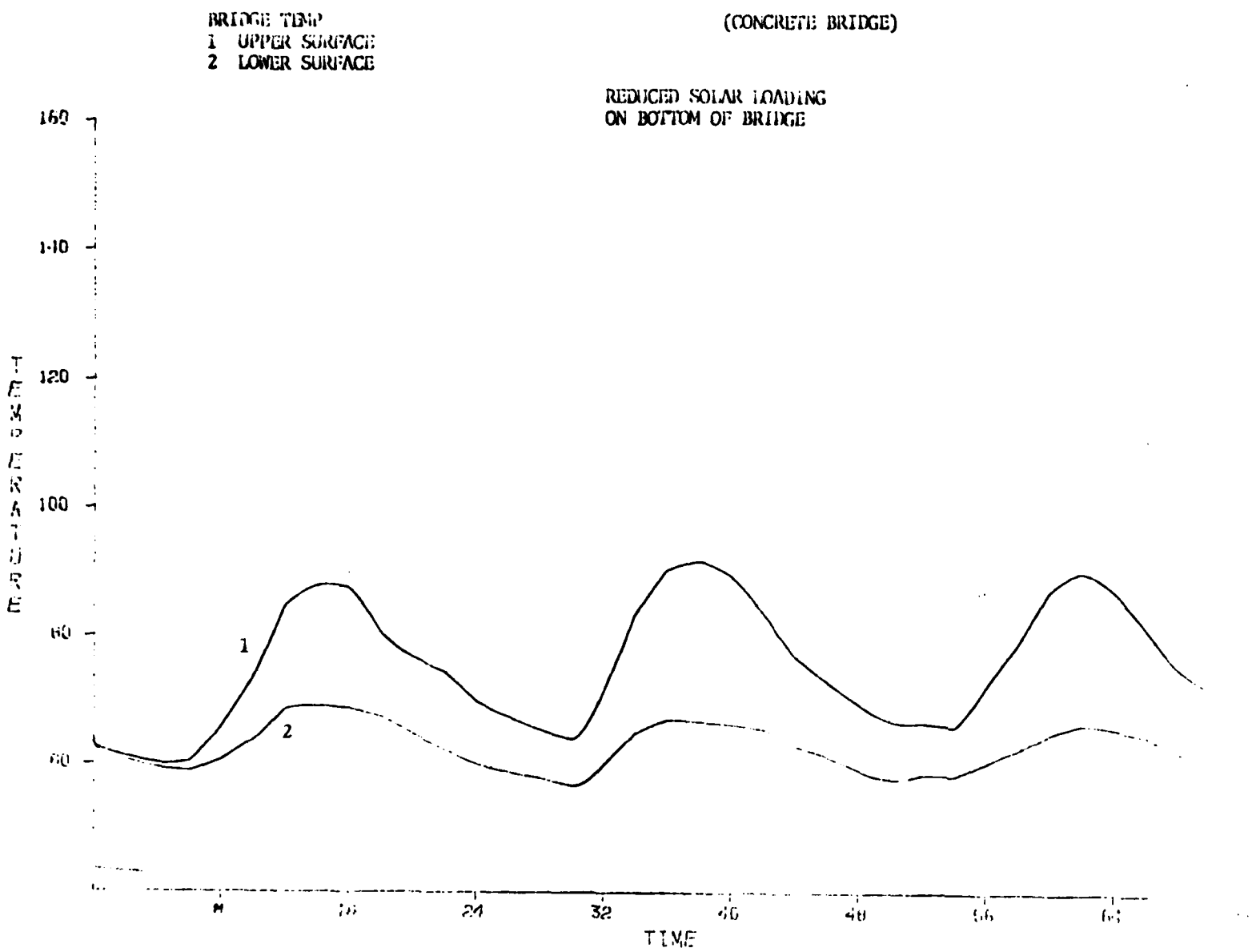

Figure 15. Temperature Profile for Bridge - Real Summer Environmental Data

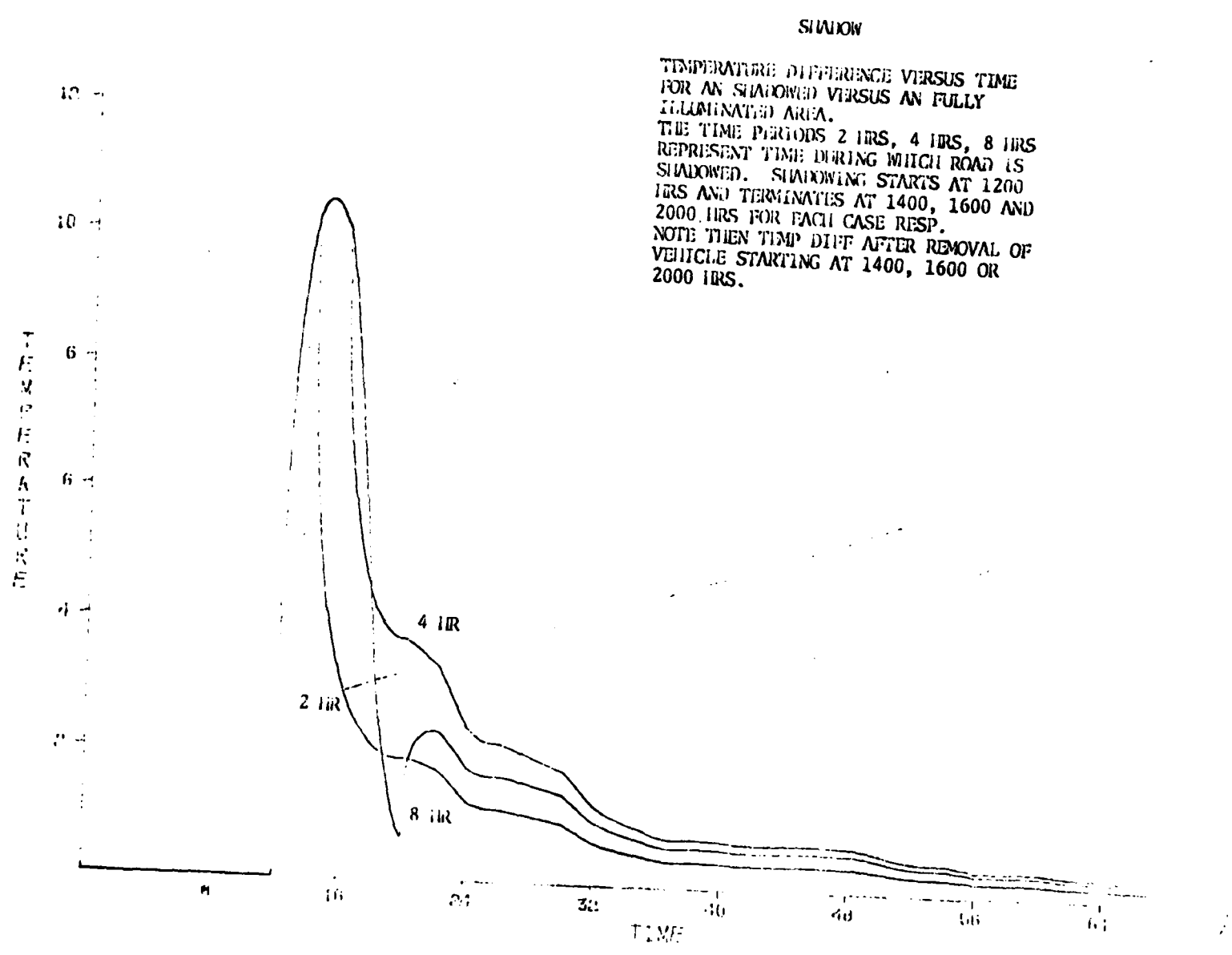

Figure 16. Shadow Curves - Real Summer Environmental Data

SECTION V

CONCLUSIONS

The model as presently configured appears to be a useful tool for prediction of background surface temperatures. The background can include both natural terrain and man-made features.

The formulations when implemented in the model seem to give profiles with reasonable excursions in temperature considering the external environmental conditions.

The solar energy and wind inputs seem to be the principle driving functions effecting surface temperatures. Correlation of temperature changes with changes in both these variables is evident particularly for low thermal inertia features.

The finite difference method for calculation of temperatures in large thermal inertia targets seems to give reasonable values with ten vertical intervals per layer of material. Increasing the number of intervals beyond this value seemed to have only negligible effect on calculated temperature values.

The assumption of isolated elements for the vegetation model would seem to predict temperature values that are lower than actual measured values. This is based upon the conjecture that the radiated energy from biomass surrounding each vegetative element would tend to increase the temperature of each radiating surface.

The present method for representation of small active targets, while quite simplified, is adequate for temperature prediction in key hotspots (hood, top, etc) of vehicle.

However, an accurate prediction of target detection against a complex background would require temperature profile over target region which, in turn, would require a representation and modeling based upon full spatial and angular extent of target surfaces and corresponding interaction with thermal environment.

REFERENCES

1. D. Bornemeir, M. Mennet, R. Horvath, Target Temperature Modeling, RADC-TR-69-404, December 1969.

2. William D. Sellers, Physical Climatology View of Chicago Press, 1965.

3. Ronald F. Scott, "Estimation of the Heat Transfer Coefficient Between Air and Ground Surface," Transaction, American Geophysical Union, February 1957.

4. K. Roschke, "Heat Transfer Between Plant and Environment," Annual Review Plant Physiology Vol II 1960.

5. The Infrared Handbook, 1978.

6. P. Bannister, Introduction to Physiological Plant Ecology, New York, John Wiley, Hotstead Press. Blackwell Scientific Publication - Chapters 2 and 3.

7. D. A. Kiner and J. A. Smith, "Simulation of Solar Radiation Absorption in Vegetation Canopies," Applied Optics Vol 19 August 15, 1980.

8. "Temperatures of Dessert Plants: Another Perspective on the Adaptability of Leaf Size," Science, Vol 201, 18 August 1978.